CLIN. EXPL. METASTASIS, 1984, VOL. 2, NO. 4, 333–355

Multiple phenotypic divergence of mammary adenocarcinoma cell clones

I. *In vitro* and *in vivo* properties

DANNY R. WELCH†§‖, DAVID B. KRIZMAN‡§
and GARTH L. NICOLSON†¶

Departments of †Tumor Biology and ‡Genetics,
The University of Texas–M. D. Anderson Hospital and Tumor Institute,
and The University of Texas Health Science Center,
§Graduate School of Biomedical Sciences, Houston, Texas 77030, U.S.A.

(*Received 27 July 1984; accepted 26 August 1984*)

The properties of cell clones derived from locally growing and spontaneous metastases of 13762NF mammary adenocarcinoma change during *in vitro* growth. This has been termed phenotypic drift and is reproducible in independent experiments using different cryoprotected cell stocks. To determine whether phenotypic drift in 13762NF cell clones is the result of an *en bloc* shift in the properties of all tumor cells, or independent phenotypic divergence of tumor cells to produce a mixed cell population, local tumor-derived clone MTF7 was subcloned at low and high culture passage numbers *in vitro*. Each subclone was analyzed *in vitro* for cell morphology, growth rate, saturation density, karyotype and ploidy, and *in vivo* for experimental metastatic behavior. Subclones derived from low passage clone MTF7 (T11; tissue culture passage number 11) were relatively homogeneous in their growth rates (doubling times of 16·8–17·4 h) and saturation densities ($\sim 2 \times 10^5$ cells/cm^2); yet, these same subclones were heterogeneous in their *in vitro* cell morphologies, experimental metastatic potentials (means range from 0 to >100 tumor nodules per lung), size distributions of lung tumor nodules, marker chromosomes and modal chromosome numbers. High passage MTF7 (T35; tissue culture passage number 35) subclones had similar growth rates and saturation densities, except for subclone 2, which had a doubling time of ~ 26 h. Cell morphologies, experimental metastatic potentials (means range from 3 to >600 tumor nodules per lung), size distribution of lung tumor nodules, marker chromosomes and modal chromosome numbers varied between MTF7 (T35) subclones. The results suggest that simultaneous, independent divergence of several phenotypes from a single cloned cell occurred to form a mixed cell population containing cells with independently segregated, unrelated phenotypes. Thus, the reproducibility of phenotypic drift in clonal cell populations was probably the result of tumor cell divergence and was not an *en bloc* shift in phenotypic properties of all cells.

Introduction

Heterogeneity exists at a minimum of three levels in malignant neoplasms: (i) between individual tumors of the same histological classification in different hosts; (ii) between individual tumors and their metastases of the same histologic classification in a single host; and (iii) between individual cells within the same

‖ Present address: Cancer Research, The Upjohn Company, Kalamazoo, Michigan 49001, U.S.A.

¶ To whom reprint requests should be addressed.

tumor. The importance of such tumor heterogeneity to the success of cancer therapy is obvious, because effective therapeutic measures that do not eliminate virtually all tumor cells, including those with diverse metastatic and therapy-resistant phenotypes, may fail to control seemingly curable neoplasms [25, 31, 40].

The vast majority of tumors happen to arise from a single transformed cell [4, 27]. However, at the time of diagnosis, tumor progression and diversification can ensure the evolution of multiple, phenotypically distinct cell subpopulations [8, 22, 23, 27, 31]. Heterogeneity in the properties of malignant cells has been described for: (i) metastic potential, (ii) metastatic profile and site of metastatic colonization, (iii) cell surface properties, (iv) immunogenicity and host responses, (v) *in vivo* cell morphology, (vi) karyotype, (vii) cell adhesive properties, (viii) cell enzymes, and (ix) response to chemotherapy, hyperthermia and ionizing radiation [reviewed in 10, 11, 17, 20–26, 31, 32, 35].

The growth of a single tumor cell clone *in vitro* or *in vivo* can apparently result in rapid diversification of subpopulations that possess differing metastatic behavior [3, 16, 18, 32–34], biochemical properties [9, 16, 39] and sensitivity to various therapeutic modalities [41, 42, 44, 46]. The shift in cellular characteristics associated with culture or *in vivo* passage has been termed *phenotypic drift* [18]. Poste *et al.* [33–34] and Miner *et al.* [16] have shown that phenotypic drift in metastatic properties of B16 melanoma cells is the result of cell clonal population divergence during growth. In contrast to the instability seen in clonal populations, polyclonal mixtures remained stable for prolonged periods of growth. In some tumor systems, such as the 13762NF mammary adenocarcinoma, phenotypic drift is reproducible for individual cell clones. This can be tested using different cryoprotected stocks of cells at dissimilar passage numbers. As long as the 13762NF cells are assayed at the same final passage number, the magnitude and the direction of the phenotypic shift is identical. For example, local tumor-derived clone MTC is poorly metastatic and radioresistant at low (T11; tissue culture passage number 11) *in vitro* passage numbers [18, 19, 44]. When the cells are grown to passage 20 (T20), they become increasingly metastatic [18] and the radiation dose–response curve becomes triphasic, indicating the presence of both sensitive and resistant subpopulations [44]. Reproducibility of the phenotypic changes in this and other 13762NF cloned cell lines has also been described for sensitivity to chemotherapy agents [46] and hyperthermia [41]. To determine whether the phenotypic drift of the 13762NF cells occurs via an *en bloc* shift of all cells at specific passages or by clonal cellular divergence, cell clones were subcloned at low and high *in vitro* passage numbers and examined for their *in vitro* properties, such as cell morphology, growth rate, saturation density, karyotype and ploidy, and *in vivo* properties such as growth and lung colonization potential. Similar studies on the sensitivity to drugs, ionizing radiation and hyperthermia are presented in the accompanying paper [43].

Materials and methods

Cell lines, tissue culture and photomicroscopy

Doubly cloned cell lines were derived from the 13762NF mammary adenocarcinoma tumor growing at local implant sites, (MTC, MTF7) and from spontaneous lung metastases (MTLn2, MTLn3) [19] (figure 1). Cells were grown in a 37°C humidified atmosphere (95 per cent air, 5 per cent CO_2) in alpha modified minimal

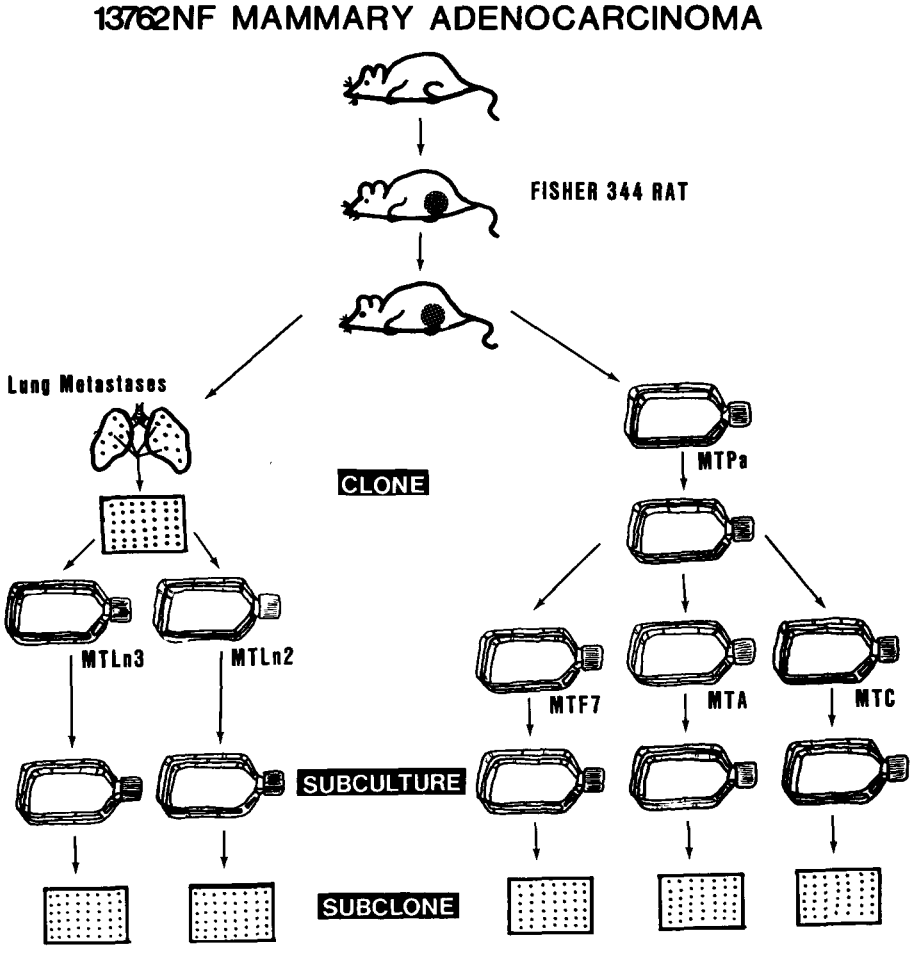

Figure 1. Establishment of 13762NF mammary adenocarcinoma cell clones and subclones.

essential medium (AMEM) without deoxyribonycleotides, nucleotides or antibiotics and containing 10 per cent fetal bovine serum (FBS) (Biocell, Carson, CA, Lot No. 209181 for initial cloning, growth curves and saturation density curves and HyClone, Lot No. 100389 for all other studies) (complete AMEM). Cells were routinely subcultured at dilution ratios of 1:50 (MTC and MTF7) or 1:150 (MTLn2 and MTLn3) when the tissue culture dishes or flasks (Corning Plastic Div., Corning, NY) became ~80 per cent confluent.

Cells were frozen at various *in vitro* passage numbers in liquid nitrogen at a rate of −1°C/min using a programmed cell freezer (Cryomed, Model 900, Mt Clemens, MI). The cells were stored in Dulbecco's phosphate-buffered saline (DPBS) containing 20 per cent FBS and 10 per cent dimethylsulfoxide (DMSO) at a concentration of $3–5 \times 10^6$ cells/ml in Nunc freezing vials. Frozen samples were quickly thawed in a 37°C water bath, removed with a wide bore 1 ml plastic serologic pipet and placed into five 100 mm tissue culture dishes containing 15 ml of prewarmed complete AMEM. After 12–16 h, the medium was aspirated and

replaced with prewarmed complete AMEM. Viability was always greater than 90 per cent, and cells were generally used 2–4 days after thawing.

Phase contrast micrographs were prepared using a Nikon Diaphot phase contrast microscope with 10 × and 20 × objectives. Low density and high density cultures were washed twice with warm DPBS and pictures were taken with DPBS present in the dishes.

Cell cloning

Cell clones were trypsinized (0·25 per cent trypsin in calcium, magnesium-free DPBS (CMF-DPBS) and resuspended in ice cold complete AMEM at a concentration of 0·20–0·33 cells/ml. The cells were seeded (0·2 ml/well) into Corning flat-bottom 96-well tissue culture dishes. After 14–16 h, each well was examined by phase microscopy and scored for the presence of a single cell. Wells that contained only one cell at the initial examination were expanded for freezing and experimentation. Random clones were chosen for characterization. The nomenclature for each clone is of the following form: MTC(TX).Y(TZ), where MT designates that the cells are derived from the 13762NF mammary adenocarcinoma; Y is the subclone designation, and X and Z are the numbers of clonal and subclonal culture passages, respectively. All subclone assays were performed on cells that had been passaged *in vitro* 3–5 times following subcloning.

In vitro *cell growth characteristics*

Cell growth curves were performed by plating either 5×10^4 cells or 1×10^5 cells onto Corning 60 mm diameter tissue culture dishes containing 5 ml of complete AMEM. Cell numbers were determined every 24 h by trypsinizing the dish and counting directly using a hemacytometer. Dilutions, if necessary, were made by addition and resuspension in ice-cold CMF-DPBS. Saturation density was determined as above, except that the medium was changed daily after 72 h.

Determination of cell ploidy and karyotype

Subclones with low, intermediate and high metastatic potentials were selected for karyotypic analysis. The cells were harvested from subconfluent cultures after treatment with Colcemid (2 μg/ml) for 30 min at 37°C. The mitotic cells were detached with 0·01 per cent trypsin, and after 5 min were resuspended in complete AMEM. The cell suspension was centrifuged, and the pellet resuspended and incubated in 0·075 M potassium chloride for 20 min at room temperature. Carnoy's fixative (3 : 1 methanol : acetic acid) (1 ml) was added, the sample was centrifuged and then washed three times by resuspension in the fixative solution. The fixed cells were spread onto clean wet slides and dried at room temperature for at least 3 weeks. The mitotic chromosomes were stained with a 4 per cent Giemsa solution in 0·01 M sodium phosphate buffer [29].

Animals

Syngeneic, age-matched (7–8 weeks) female Fischer 344 rats (F344/CRBL, Charles River Breeding Laboratories, Portage, MI) were used for all experiments. Animals were certified virus- and pathogen-free and were shipped in filtered cages. Upon arrival, the animals were maintained under the guidelines of the National Institutes of Health and The University of Texas System Cancer Center, and were quarantined for 1 week. All animals were routinely screened for pathogens and were

found to be free of infections. They were fed normal rat chow (Purina Rodent Chow, 5001, Ralston Purina Co.) and acidified water (less that 2 p.p.m. chlorine) *ad libidum*.

Analysis of experimental lung metastasis data

Lung metastases were quantitated as described previously [45]. Briefly, surface lung nodules were counted and placed into three volume categories: small volumes (SVol) of <1 mm in diameter (average radius $=0{\cdot}25$ mm), medium volumes (MVol) of 1–3 mm in diameter (average radius $=0{\cdot}75$ mm), and large volumes (LVol) of >3 mm diameter (radii and volumes calculated individually). Tumor volumes were calculated based on the formula: $V=[(4/3)r^3]\times N$ where V is the volume of each group of lung nodules, r is the average radius and N is the number of individual lung lesions per group. Total lung metastases volume (TVol) is the sum of volumes calculated for each group.

Experimental metastasis assays

Tumor cells were detached from subconfluent cultures using 0·25 per cent trypsin in CMF-DPBS. The medium was aspirated, and 1 ml of ice-cold trypsin solution was added and removed immediately. Another 1 ml of trypsin solution was added, and each dish was placed into a 37°C humidified incubator until the cells began to detach. Trypsin solution was inactivated by suspending the detached cells in ice-cold complete AMEM in polypropylene centrifuge tubes. The suspended cells were pelleted by low speed centrifugation, the medium was aspirated, and the cells were resuspended in ice-cold AMEM. Cell concentrations were adjusted by addition of AMEM to a final concentration of 5×10^4 viable cells/0·2 ml; cell counts and viabilities were determined with a hemacytometer using the trypan blue dye-exclusion method. The tube containing the cell suspension was maintained in an ice bath, and 5×10^4 cells/0·2 ml were injected into the lateral tail vein of age- and sex-matched rats. Total time for injection of 15 animals was less than 15 min.

Results

Six subclones from local tumor-derived clone MTF7 (T11) and MTF7 (T35), seven subclones from local tumor-derived clone MTC (T22), and four subclones from lung metastasis-derived clone MTLn3 (T44) were obtained by the limiting dilution cell cloning method (figure 1). In all cases, plating efficiency was >90 per cent. Detailed data for subclones isolated from MTF7 are discussed here, but experimental metastasis results and *in vitro* growth data are also included for subclones derived from clones MTC and MTLn3.

In vitro *cell morphologies*

Phase contrast micrographs of low and high density tissue cultures of clones MTF7 (T11) and MTF7 (T35) (figure 2) and their respective subclones (figures 3–6) showed that all of the subclones generally retained the spindlar epithelial morphology characteristic of clone MTF7. These cells tended to aggregate and plate as cell clumps rather than single cells, unless precautions were taken to ensure a uniform, single cell distribution. Low passage-derived subclones MTF7 (T11).2, MTF7 (T11).3 and MTF7 (T11).13 initially attached as single cells or small cell aggregates and exhibited polygonal morphologies (figures 3 and 4). As the cells became more dense, they developed more polarized morphologies with increased numbers of cytoplasmic projections. Subclones MTF7 (T11).2 retained a more

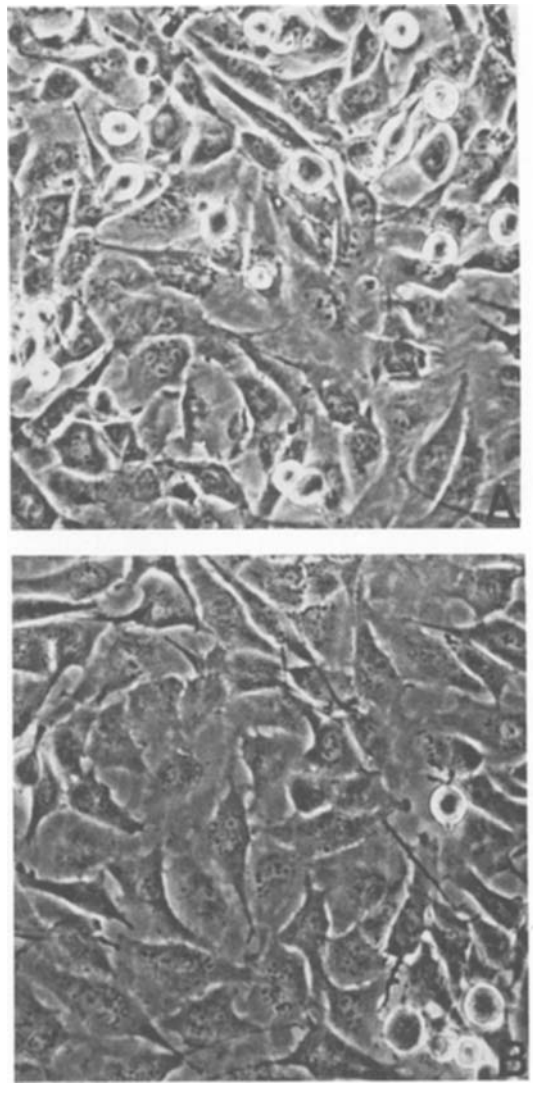

Figure 2. *In vitro* phase contrast micrographs of cell clone MTF7 used for subcloning. A, MTF7 (T11); B, MTF7 (T35). Magnification, 150×.

apparent polygonal morphology than the other MTF7 (T11) subclones, while subclones MTF7 (T11).1, MTF7 (T11).4 and MTF7 (T11).7 initially plated as single, spindlar cells with several cytoplasmic extensions. In addition, subclones MTF7 (T11).1 and MTF7 (T11).4 initially plated so that the cells grew in a 'swirling' pattern reminiscent of normal fibroblasts. Subclone MTF7 (T11).7 cells grew in a parallel configuration, and this basic pattern remained as the cells became more confluent. Subclone MTF7 (T11).1 cells became more dense than shown in figure 3 B, and there was a tendency for these cells to detach at high cell densities. All of the cells from the MTF7 (T11) subclones exhibited some cytoplasmic, but little nuclear, overlapping. As the cells become more confluent, they generally arranged to form more compact and structured patterns.

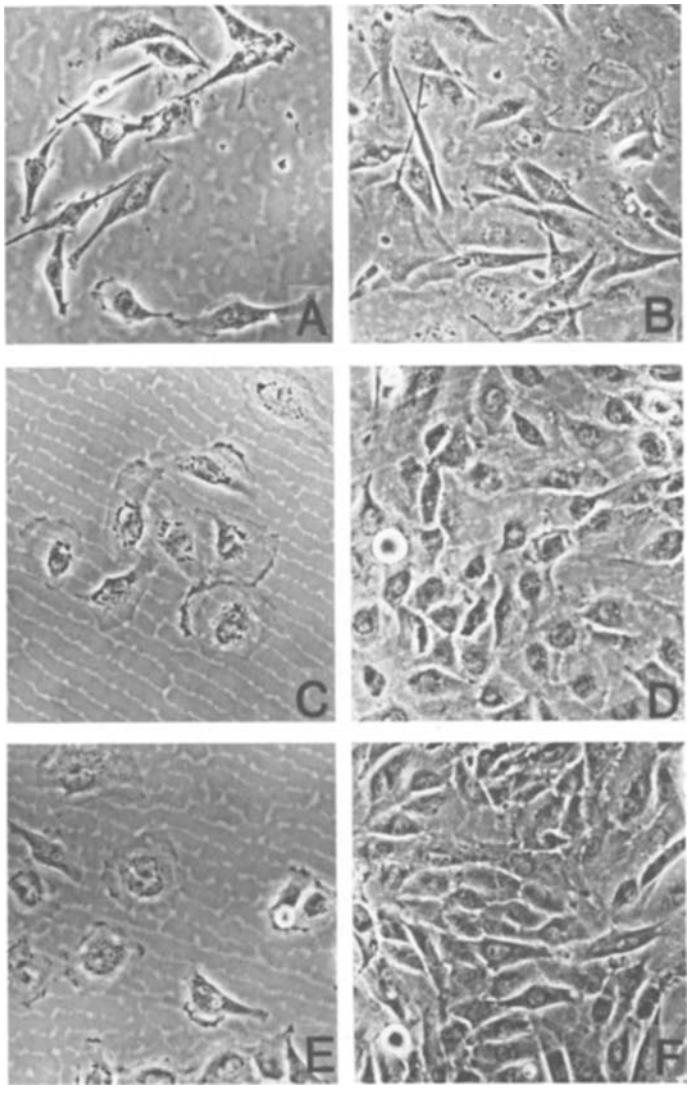

Figure 3. *In vitro* phase contrast micrographs of MTF7 (T11) subclones at low (A, C, E) and high (B, D, F) cell density. A and B, MTF7 (T11).1; C and D, MTF7 (T11).2; E and F, MTF7 (T11).3. Magnification, 150×.

Generally, the cells from high passage-derived MTF7 (T35) subclones initially attached and spread as polarized cells with numerous cytoplasmic projections (figures 5 and 6). As in the MTF7 (T11) subclones, there was little nuclear, but some cytoplasmic, overlapping of the cells at high densities. Subclones MTF7 (T35).1 and MTF7 (T35).5 cells formed highly organized epithelial nonolayers with 'swirling' patterns at high densities, while subclone MTF7 (T35).3 cells formed organized confluent monolayers with more cytoplasmic overlap and a higher percentage of multinucleated cells than the other subclones. Subclone MTF7 (T35).2 cells formed long cytoplasmic extensions that sometimes spanned several cell diameters. There

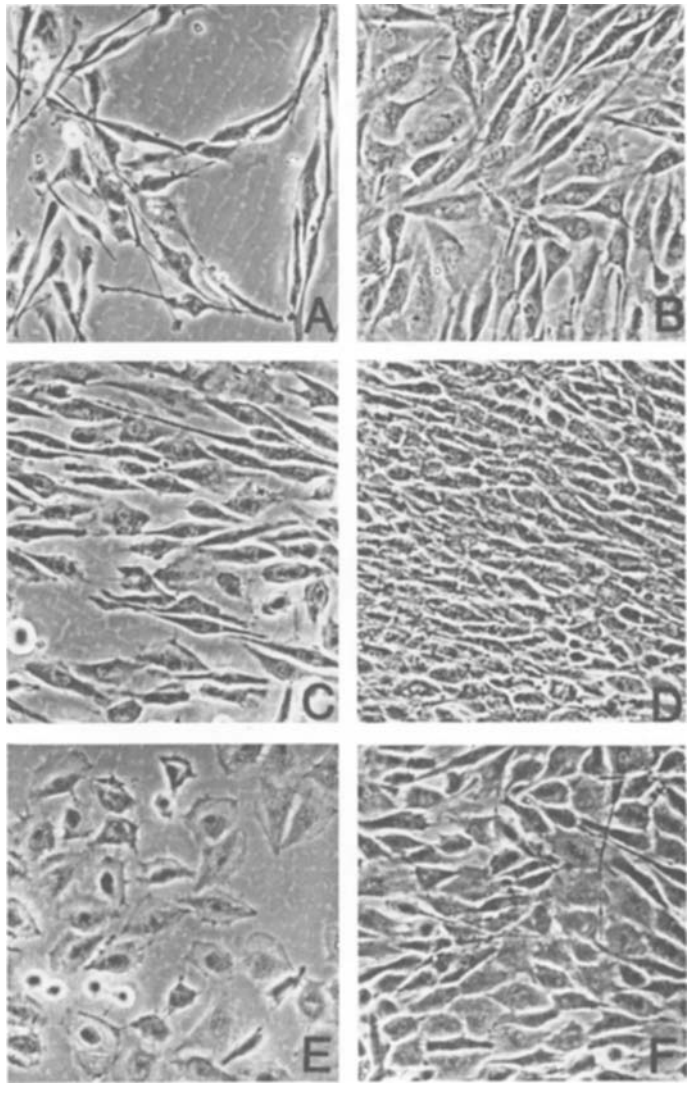

Figure 4. *In vitro* phase contrast micrographs of MTF7 (T11) subclones at low (A, C, E) and high (B, D, F) density. A and B, MTF7 (T11).4; C and D, MTF7 (T11).7; E and F, MTF7 (T11).13. Magnification, 150×.

was increased nuclear overlap by these cells, and they were frequently arranged around a cell with flattened morphology. Cells of all of the MTF7 (T35) subclones were highly pleiomorphic at low cell densities, and became more organized and uniform as the cultures became more confluent.

In vitro *cell growth kinetics and saturation densities*

MTF7 (T11) and MTF7 (T35)-derived subclones had *in vitro* doubling times between 16·8 and 17·4 h, except for MTF7 (T35).2 cells which had a doubling time of 26 h (table 1 and figure 7). The rate of *in vitro* tumor cell growth was unchanged if the

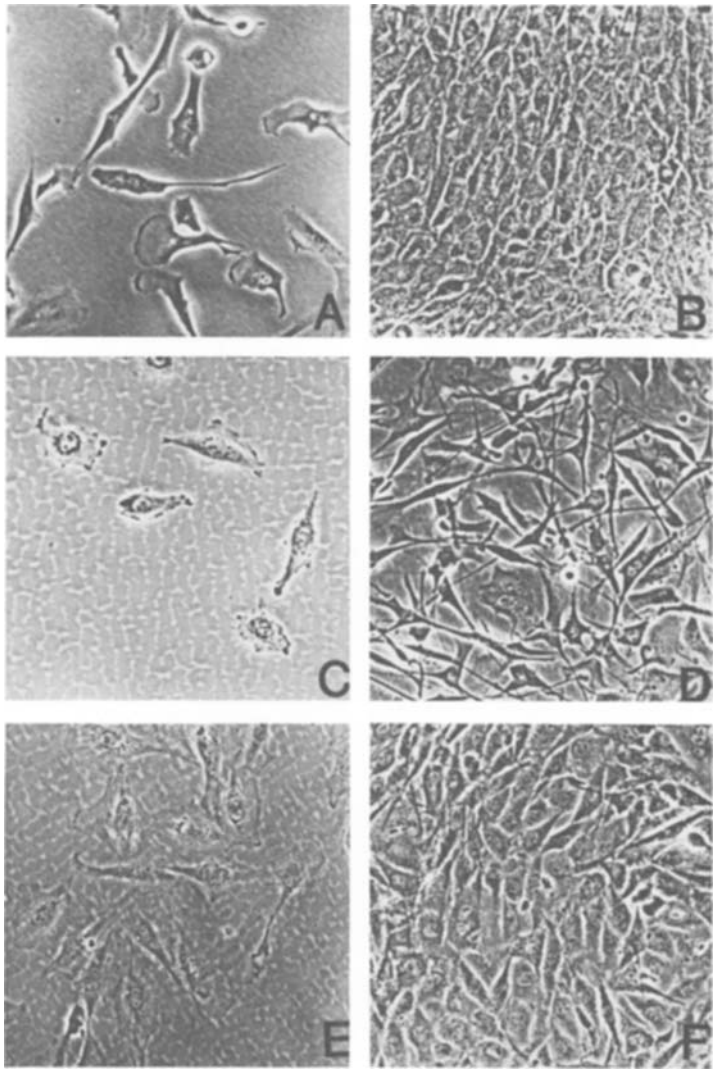

Figure 5. *In vitro* phase contrast micrographs of MTF7 (T35) subclones at low (A, C, E) and high (B, D, F) density. A and B, MTF7 (T35).1; C and D, MTF7 (T35).2; E and F, MTF7 (T35).3. Magnification, 150×.

medium was replaced daily beginning at 72 h; however, the cell numbers at confluency (saturation density) increased (figure 7), and they generally exhibited densities of approximately 2×10^5 cells/cm^2.

Experimental metastasis assays

Each of the subclones was tested for its experimental metastatic potential following i.v. injections of 5×10^4 cells into the lateral tail vein. A wide range of metastatic potentials was observed for both the number and volume of metastatic lung lesions for subclones derived from clones MTF7 (T11) and MTF7 (T35)

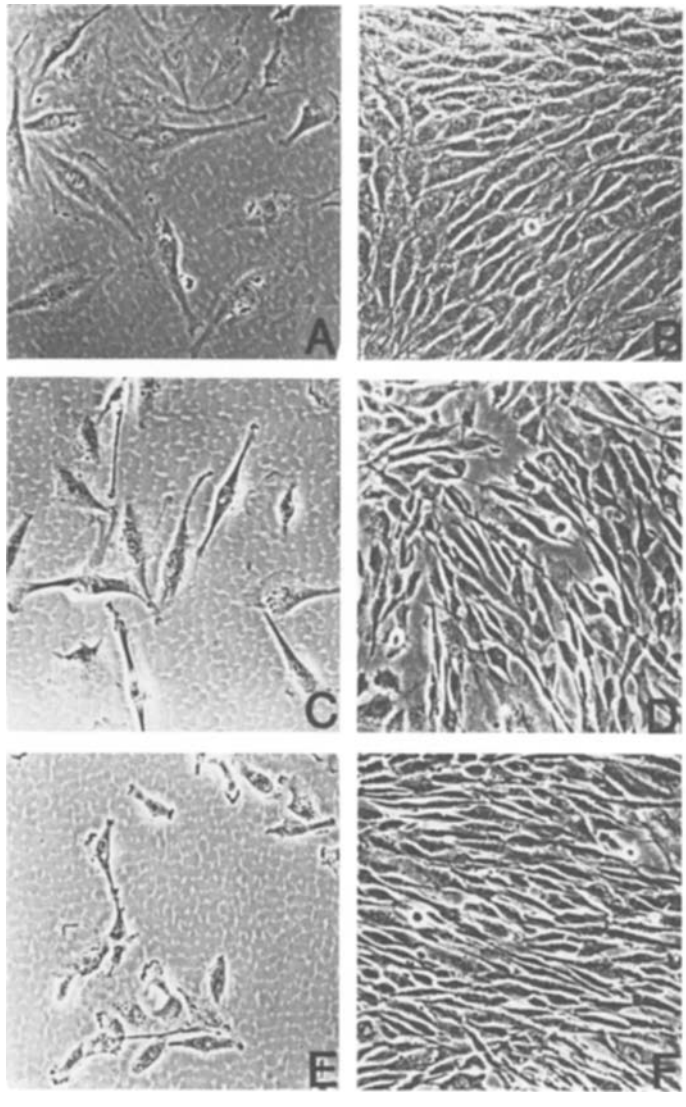

Figure 6. *In vitro* phase contrast micrographs of MTF7 (T35) subclones at low (A, C, E) and high (B, D, F) density. A and B, MTF7 (T35).5; C and D, MTF7 (T35).6; E and F, MTF7 (T35).7. Magnification, 150×.

(tables 2–5). MTF7 (T11) subclones ranged from poorly metastatic (average of 6·2 lesions/lung, and 3·4 mm^3 lung tumor burden) to intermediate metastatic potential (average of 147 lesions/lung, and 97 mm^3 lung tumor burden) (table 2). As seen previously with 13762NF clonal populations [45], each subclone exhibited a characteristic pattern for the number and size of lung metastases (table 6 and figure 8). For example, subclone MTF7 (T11).1 had approximately the same lung colonization potential as subclone MTF7 (T11).7; yet, the proportion of lung foci of different sizes was dramatically different. In the former, total lung tumor volume was ~63 per cent small tumor nodules (< 1 mm in diameter) and ~37 per cent medium-sized nodules (between 1 and 3 mm in diameter), while lung tumor burden of the

Table 1. Growth kinetics of 13762NF mammary adenocarcinoma subclones.

Subclone	Doubling time[a] (h)	Saturation density[b] (cells/cm^2)
MTF7 (T11).1 (T3–T5)	17	$2{\cdot}19 \times 10^5$
MTF7 (T11).2 (T3–T5)	17	$1{\cdot}78 \times 10^5$
MTF7 (T11).3 (T3–T5)	17	$1{\cdot}55 \times 10^5$
MTF7 (T11).4 (T3–T5)	17	$1{\cdot}85 \times 10^5$
MTF7 (T11).7 (T3–T5)	17	$1{\cdot}23 \times 10^5$
MTF7 (T11).13 (T3–T5)	17	$1{\cdot}85 \times 10^5$
MTF7 (T35).1 (T3–T5)	17	$2{\cdot}19 \times 10^5$
MTF7 (T35).2 (T3–T5)	26	$1{\cdot}90 \times 10^5$
MTF7 (T35).3 (T3–T5)	16	$2{\cdot}10 \times 10^5$
MTF7 (T35).5 (T3–T5)	16	$1{\cdot}90 \times 10^5$
MTF7 (T35).6 (T3–T5)	17	$1{\cdot}90 \times 10^5$
MTF7 (T35).7 (T3–T5)	17	$2{\cdot}24 \times 10^5$
MTC (T22).1 (T3–T5)	17	$1{\cdot}52 \times 10^5$
MTC (T22).3 (T3–T5)	17	$2{\cdot}14 \times 10^5$
MTC (T22).5 (T3–T5)	18	$2{\cdot}14 \times 10^5$
MTC (T22).6 (T3–T5)	17	$2{\cdot}67 \times 10^5$
MTC (T22).7 (T3–T5)	19	$2{\cdot}76 \times 10^5$
MTC (T22).9 (T3–T5)	17	$1{\cdot}48 \times 10^5$
MTC (T22).10 (T3–T5)	19	$2{\cdot}19 \times 10^5$
MTLn3 (T44).4 (T3–T5)	17	$4{\cdot}27 \times 10^5$
MTLn3 (T44).5 (T3–T5)	14	$4{\cdot}65 \times 10^5$
MTLn3 (T44).9 (T3–T5)	14	$4{\cdot}93 \times 10^5$
MTLn3 (T44).11 (T3–T5)	17	N.D.[c]

[a] Cells were grown on Corning 60 mm tissue culture dishes and counted each day using a hemacytometer.

[b] Same as above except media was changed every 24 h beginning at 72 h.

[c] Not determined.

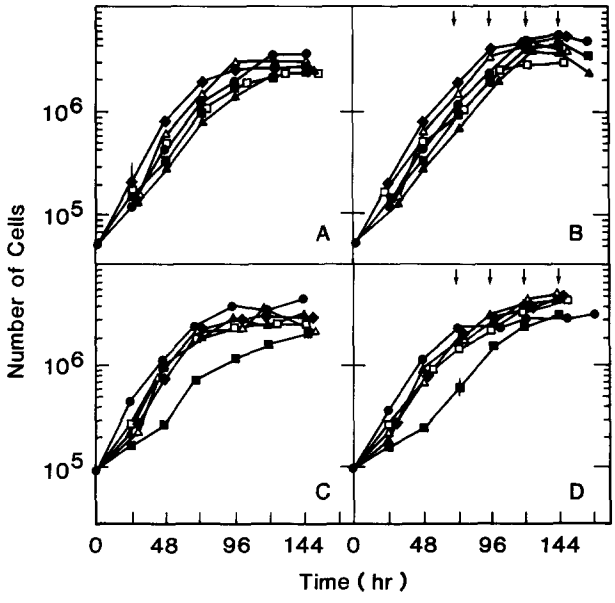

Figure 7. *In vitro* growth (A and C) and saturation density (B and D) curves for MTF7 low and high passage-derived subclones. A and B, MTF7 (T11).1 (●); MTF7 (T11).2 (■); MTF7 (T11).3 (▲); MTF7 (T11).4 (□); MTF7 (T11).7 (◆); and MTF7 (T11).13 (△). C and D, MTF7 (T35).1 (●); MTF7 (T35).2 (■); MTF7 (T35).3 (▲); MTF7 (T35).5 (□); MTF7 (T35).6 (◆); and MTF7 (T35).7 (△). Data points are mean ±S.D.

Table 2. Experimental metastatic potential of 13762NF mammary adenocarcinoma MTF7 (T11) subclones[a]

Clone or subclone	No. rats with lung metastasis/ total no.	Volume of lung metastases[b]				Number of lung nodules (95 per cent C.I.)
		TVol (95 per cent C.I.)[d]	SVol (95 per cent C.I.)	MVol[c] (95 per cent C.I.)	LVol (95 per cent C.I.)	
MTF7 (T11)		7·25 (3·88, 10·62)[d]	3·15 (1·75, 4·56)	3·33 (1·66, 5·01)	0·76 (0, 2·30)	50·09 (27·91, 72·27)
cl.1	43/43	97·32 (82·04, 112·60)	60·91 (51·85, 69·97)	36·08 (28·90, 43·26)	0·33 (0, 0·99)	136·77 (116·17, 157·37)
cl.2	43/43	31·33 (24·20, 38·46)	25·53 (19·18, 31·89)	5·79 (4·26, 7·33)	0 (—)	52·05 (39·53, 64·57)
cl.3	41/47	3·40 (2·27, 4·53)	3·32 (2·20, 4·15)	0·23 (0, 0·46)	0 (—)	6·19 (4·25, 8·13)
cl.4	30/30	6·09 (3·75, 8·42)	5·60 (3·41, 7·59)	0·59 (0·19, 0·99)	0 (—)	10·83 (6·71, 14·95)
cl.7	43/43	86·21 (71·84, 100·59)	73·30 (61·06, 85·55)	12·41 (9·75, 15·07)	0·50 (0, 1·50)	147·04 (122·74, 171·35)
cl.13	45/45	8·19 (5·99, 10·39)	7·25 (5·28, 9·21)	0·95 (0·44, 1·45)	0 (—)	14·37 (10·51, 18·24)

[a] 5×10^4 cells were injected into lateral tail vein of syngeneic F344/CRBL rats. Lung metastases were quantitated 23 days post-inoculation.

[b] Lung volumes (mm^3) were calculated according to Welch *et al.* [45]. SVol refers to volume of lung metastases produced by nodules less than 1 mm in diameter; MVol-greater than 1 mm but less than 3 mm in diameter; LVol-diameters greater than 3 mm in diameter; TVol equals total volume of lung metastases.

[c] Average diameter = 1·5 mm.

[d] 95 per cent confidence interval, computed using propagation of error.

Table 3. Experimental metastatic potential of 13762NF mammary adenocarcinoma MTF7 (T35) subclones[a].

Clone or subclone	No. rats with lung nodules/ total no.	Volume of lung metastases[b]				Number of lung nodules (95 per cent C.I.)
		TVol (95 per cent C.I.)[d]	SVol (95 per cent C.I.)	MVol[c] (95 per cent C.I.)	LVol (95 per cent C.I.)	
MTF7 (T35)		11·58 (6·78, 16·37)[d]	5·36 (3·50, 7·21)	3·57 (1·38, 5·76)	2·65 (0, 5·84)	83·92 (55·18, 112·66)
cl.1	25/25	487·52 (431·15, 543·88)	230·36 (214·53, 246·19)	246·18 (201·90, 291·06)	10·67 (4·30, 17·05)	579·96 (530·53, 629·39)
cl.2	24/24	73·78 (63·12, 84·45)	69·66 (59·33, 79·99)	4·12 (3·03, 5·22)	0 (—)	135·38 (115·47, 155·28)
cl.3	27/27	596·20 (543·62, 648·78)	207·79 (201·43, 214·15)	366·58 (318·92, 414·25)	21·82 (10·47, 33·18)	605·44 (573·83, 637·06)
cl.5	27/27	143·70 (113·58, 173·82)	143·50 (113·29, 173·72)	0·20 (0, 0·42)	0 (—)	274·19 (216·54, 331·83)
cl.6	27/27	67·26 (57·18, 77·34)	66·15 (56·01, 76·28)	1·11 (0·44, 1·79)	0 (—)	126·96 (107·65, 146·28)
cl.7	18/27	1·61 (0·93, 2·29)	1·61 (0·93, 2·29)	0 (—)	0 (—)	3·07 (1·78, 4·37)

[a] 5×10^4 cells were injected into the lateral tail vein of syngeneic F344/CRBL rats. Lung metastases were quantitated 23 days post-inoculation.

[b] Lung volumes (mm^3) were calculated according to Welch *et al.* [45]. SVol refers to volume of lung metastases produced by nodules less than 1 mm in diameter; MVol-greater than 1 mm but less than 3 mm in diameter; LVol, diameters greater than 3 mm in diameter; TVol equals total volume of lung metastases.

[c] Average diameter = 1·5 mm.

[d] 95 per cent confidence interval, computed using propagation of error.

Table 4. Experimental metastatic potential of 13762NF mammary adenocarcinoma MTLn3 (T44) subclones[a].

Clone or subclone	No. rats with lung nodules/ total no.	Volume of lung metastases[b]				number of lung nodules (95 per cent C.I.)
		TVol (95 per cent C.I.)[d]	SVol (95 per cent C.I.)	MVol[c] (95 per cent C.I.)	LVol (95 per cent C.I.)	
MTLn3 (T44)		226·30 (116·12, 336·48)[d]	5·30 (3·46, 7·14)	175·08 (90·89, 259·26)	45·93 (15·53, 76·32)	102·95 (67·67, 138·23)
cl.4	17/17	422·67 (292·83, 552·50)	32·43 (16·99, 47·88)	232·92 (157·84, 308·01)	157·31 (87·71, 226·91)	54·20 (0, 132·74)
cl.5	18/18	1017·60 (823·79, 1211·41)	173·86 (116·06, 231·67)	615·86 (498·20, 733·53)	227·87 (135·78, 319·97)	436·33 (0, 1152·30)
cl.9	18/18	91·37 (34·20, 148·54)	12·86 (0, 27·72)	51·36 (27·60, 75·12)	27·15 (0, 56·55)	175·44 (0, 495·54)
cl.11	12/12	137·01 (86·96, 187·06)	9·86 (5·84, 13·88)	100·22 (53·99, 146·45)	26·93 (4·96, 48·91)	17·33 (0, 70·63)

[a] 5×10^4 cells were injected into the lateral tail vein of syngeneic F344/CRBL rats. Lung metastases were quantitated 23 days post-inoculation.

[b] Lung volumes (mm^3) were calculated according to Welch *et al.* [45]. SVol refers to volume of lung metastases produced by nodules less than 1 mm in diameter; MVol-greater than 1 mm but less than 3 mm in diameter; LVol diameters greater than 3 mm in diameter; TVol equals total volume of lung metastases.

[c] Average diameter = 1·5 mm.

[d] 95 per cent confidence interval, computed using propagation of error.

Table 5. Experimental metastic potential of 13762NF mammary adenocarcinoma MTC (T22) subclones[a]

Clone or subclone	No. rats with lung nodules/ total no.	Volume of lung metastases[b]				Number of lung nodules (95 per cent C.I.)
		TVol (95 per cent C.I.)[d]	SVol (95 per cent C.I.)	MVol[c] (95 per cent C.I.)	LVol (95 per cent C.I.)	
MTC (T22)		0·10 (0, 0·19)[d]	0 (—)	0 (—)	0 (—)	0·18 (0, 0·36)
cl.5	5/12	0·39 (0, 0·80)	0·39 (0, 0·80)	0 (—)	0 (—)	0·67 (0, 1·47)
cl.6	3/18	0·12 (0, 0·26)	0·12 (0, 0·26)	0 (—)	0 (—)	0·22 (0, 1·29)
cl.7	0/6	0 (—)	0 (—)	0 (—)	0 (—)	0 (—)
cl.9	10/12	0·87 (0·37, 1·37)	0·87 (0·37, 1·37)	0 (—)	0 (—)	1·67 (0, 4·61)

[a] 5×10^4 cells were injected into the lateral tail vein of syngeneic F344/CRBL rats. Lung metastases were quantitated 23 days post-inoculation.

[b] Lung volumes (mm^3) were calculated according to Welch *et al.* [45]. SVol refers to volume of lung metastases produced by nodules less than 1 mm in diameter; MVol-greater than 1 mm but less than 3 mm in diameter; LVol diameters greater than 3 mm in diameter; TVol equals total volume of lung metastases.

[c] Average diameter = 1·5 mm.

[d] 95 per cent confidence interval, computed using propagation of error.

Table 6. Composition of total experimental metastatic tumor burden of 13762NF mammary adenocarcinoma subclones[a].

Clone or subclone	Percentage of total volume[b]			Percentage of total no. metastases[c]		
	SVol	MVol	LVol	S	M	L
MTC (T22)	100	0	0	100	0	0
cl.5	100	0	0	100	0	0
cl.6	100	0	0	100	0	0
cl.7	0	0	0	0	0	0
cl.9	100	0	0	100	0	0
MTF7 (T11)	43	46	10	96	4	1
cl.1	63	37	1	89	11	0
cl.2	81	18	0	95	5	0
cl.3	98	2	0	100	1	0
cl.4	92	9	0	97	3	0
cl.7	85	14	1	95	5	1
cl.13	89	12	0	97	3	0
MTF7 (35)	46	31	23	97	2	1
cl.1	47	51	2	76	24	1
cl.2	94	6	0	99	1	0
cl.3	35	61	4	66	33	1
cl.5	99	1	0	99	1	0
cl.6	98	2	0	100	1	0
cl.7	100	0	0	100	0	0
MTLn3 (T44)	2	77	20	77	20	3
cl.4	8	55	37	64	32	4
cl.5	17	61	22	69	29	2
cl.9	14	56	30	62	35	3
cl.11	7	73	20	55	37	8

[a] Animals were injected with 5×10^4 cells into the lateral tail vein of syngeneic F344/CRBL rats. Metastases were quantified 23 days post-inoculation.

[b] Volumes were calculated by the method of Welch *et al.* [45]. SVol = nodules less than 1 mm in diameter; MVol = nodules greater than 1 mm but less than 3 mm in diameter; LVol = nodules greater than 3 mm in diameter. Average diameter of MVol nodules varies by clonal population. For MTC and MTF7, the average diameter is 1·5 mm. For MTLn3 (T44), the average diameter is 2.5 mm.

[c] S refers to the percentage of nodules that are less than 1 mm in diameter; M = percentage of nodules greater than 1 mm but less than 3 mm in diameter; L = percentage of nodules greater than 3 mm in diameter.

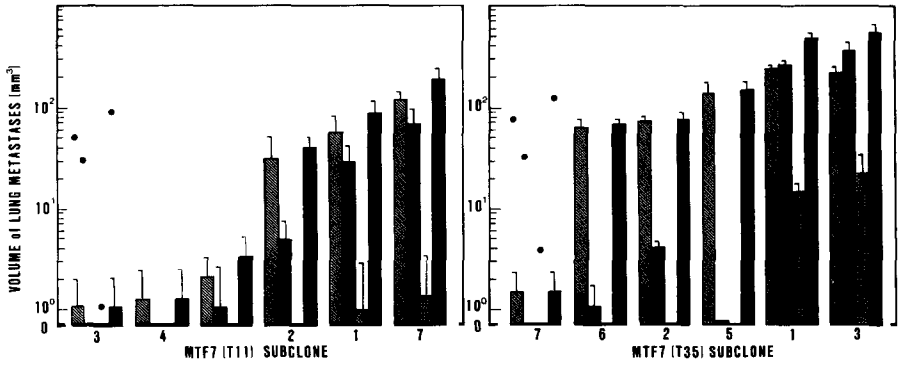

Figure 8. Comparison of the average volume distribution of experimental lung metastases formed from MTF7 subclones. Dots are mean volume for MTF7 (T11) and MTF7 (T35), respectively.

latter resulted from frequent (~85 per cent) small tumor nodules and only a small percentage of medium-sized nodules (~14 per cent).

Heterogeneity in metastatic properties was also observed for subclones derived from later passage MTF7 (T35) cells. Experimental metastatic potentials ranged from poorly metastatic (average of 3 lesions/lung, and 1·6 mm^3 tumor burden) to highly metastatic (average of >600 lesions/lung, and 596 mm^3 lung tumor burden) (table 3). Again, each subclone possessed a characteristic distribution of lung colony sizes (table 6 and figure 8).

Similar to subclones isolated from clone MTF7, subclones isolated from high passage clones MTC and MTLn3 were heterogeneous. At high passage, clone MTC remained poorly metastatic, and MTC subclones produced limited numbers of lung colonies (table 5). The MTC (T22) subclones exhibited statistically significant ($P<0·05$) differences in metastatic potentials, ranging from 0 to 1·67 metastases/lung (approximately 0·12 mm^3 lung tumor burden). All lung lesions produced by MTC (T22) subclones were less than 1 mm in diameter (table 6). Subclones derived from clone MTLn3 (T44) suggested the presence of at least four different subpopulations in MTLn3 (T44), and they were characterized by their different colonization potentials (table 4) and size distributions of metastases (table 5). The subclones ranged in experimental metastatic potential from a minimum of 175 lesions/lung and 91·4 mm^3 lung tumor burden to a minimum of 436 lesions/lung and 1017 mm^3 lung tumor burden (table 4).

Cell ploidy and karyotype

Three subclones each from low and high passage MTF7 cells and of low, intermediate and high metastatic potential were selected for karyotypic analysis and determination of their modal chromosome numbers (table 7). We found that the range of chromosome numbers was generally less in MTF7 subclones than in the 'parental' MTF7 clone [29]. The exception was subclone MTF7 (T35).7, which exhibited a bimodal, broad distribution of chromosome numbers. When ploidy was compared with metastatic potential, no correlation was found. Karyotypic evaluation indicated that the subclones possessed some, but not all, of the same marker chromosomes present in the clone MTF7 cell population and at least two new, previously undescribed marker chromosomes (figure 10).

Table 7. Ploidy of selected MTF7 subclones.

Subclone	Number of chromosomes		Metastatic potential[a]
	Mean	Range	
MTF7 (T11).2	75	71, 77	Intermediate
MTF7 (T11).3	68	66, 76	Low
MTF7 (T11).7	72	64, 72	High
MTF7 (T35).1	53, 58[b]	51, 65	High
MTF7 (T35).6	73	70, 78	Intermediate
MTF7 (T35).7	66	60, 72	Low

[a] Relative lung colonization potential following injection of 5×10^4 cells i.v. into the lateral tail vein of syngeneic F344/CRBL rats (see tables 2–5).

[b] Bimodal population with broad distribution of chromosome number.

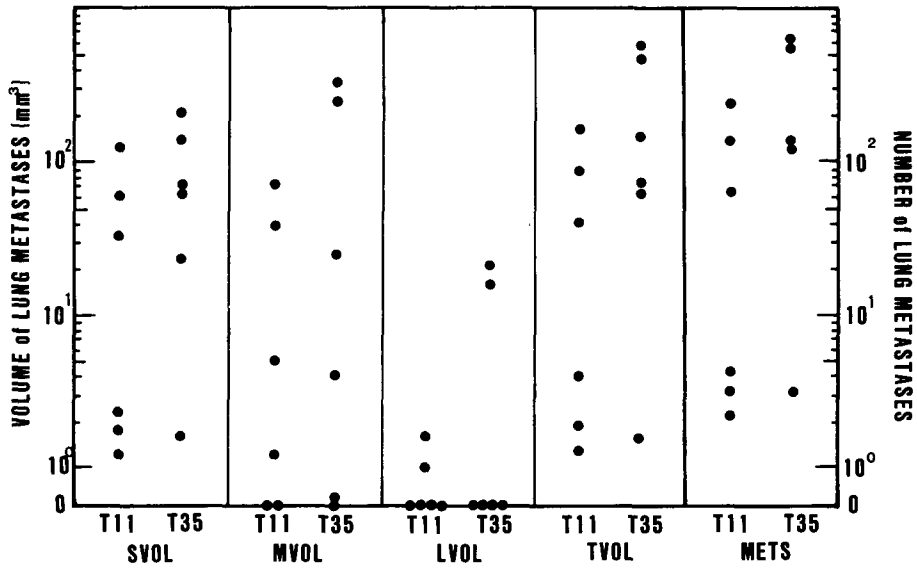

Figure 9. Experimental lung metastatic potential of MTF7 (T11) and MTF7 (T35) subclones. TVol, total metastasis volume (mm^3); SVol, volume of lung metastases produced by lesions <1 mm diameter; MVol, volume of metastases produced by nodules between 1 mm and 3 mm diameter; LVol, volume of lung metastases produced by lesions >3 mm in diameter; METS, total number of surface lung metastases. Data points are the mean value for each subclone.

Discussion

Hypotheses regarding the mechanism(s) of tumor progression have attempted to integrate observations on the inherent genetic instability of malignant cells with tumor epigenetic factors and host microenvironmental factors [7, 8, 22, 23, 27, 28]. Phenotypic drift of clonal cell subpopulations has attracted recent interest because of its possible importance in tumor progression. Several laboratories have demonstrated that phenotypic drift is the result of clonal cell divergence to form heterogeneous tumor cell populations. Poste and Greig [35] have hypothesized that this could be the mechanism responsible for development of tumor heterogeneity, and specifically in generating heterogeneity in metastatic properties.

We found previously that 13762NF mammary adenocarcinoma cell clones undergo phenotypic drift as they are grown in tissue culture for prolonged periods [18]. In our studies several phenotypic traits shifted reproducibly in magnitude and direction when assayed using different cryoprotected stocks grown to the same *in vitro* passage number. An explanation of this phenomenon was that the cloned cell lines diverged in their phenotypes with time. In support of this notion, intravenously injected tumor cells from cell clones passaged *in vitro* gave rise to lung tumor nodules with wide ranges in number and size [45]. In this system each nodule could have arisen from a cell subpopulation that possessed a unique *in vivo* growth rate. Other possibilities include: differential growth effects on tumor cells via host microenvironmental influences [22, 23, 38], metastases that formed from other metastases [36], differential homotypic aggregation of tumor cells after their intraveneous injection [2, 14], and differential tissue infiltration of tumor [20] or host cells, such as granulocytes and macrophages, into tumor lesions [13, 37].

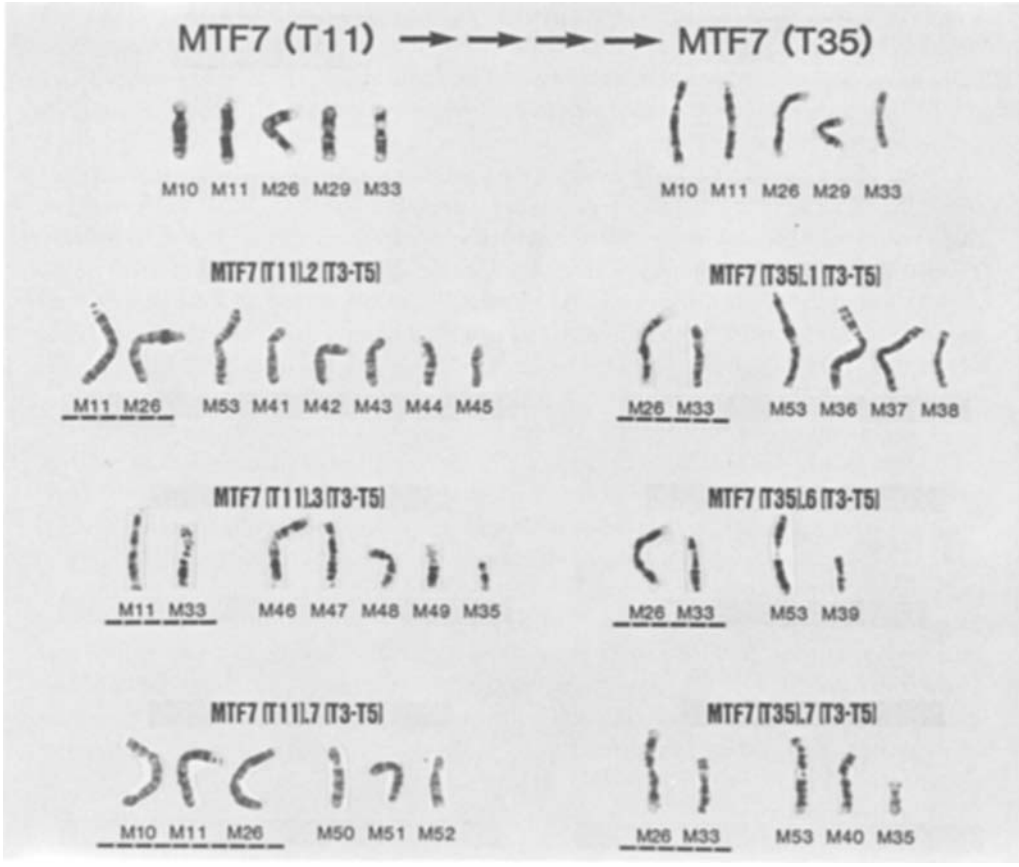

Figure 10. Marker chromosomes from 'parental' MTF7 (T11) and MTF7 (T35) clones and their respective subclones. Karyotypes were prepared from G-banded metaphase chromosomes. Only marker chromosomes are indicated here; those shared by the 'parental' MTF7 population and the subclones are underlined.

To determine whether cells from the 13762NF tumor clones randomly diverge to produce tumor cell subpopulations or shift phenotypically *en bloc*, cloned line MTF7 was subcloned at low (T11) and high (T35) *in vitro* passage numbers, and the subclones examined. Randomly selected subclones were tested for *in vitro* properties, such as cell morphology, growth rate, saturation density, karyotype and ploidy and *in vivo* properties, such as experimental metastatic potential. Experiments were conducted with subcloned cells between passages 3 and 5 to minimize diversification. By examining several tumor cell phenotypic properties simultaneously, we could determine whether the development of cellular heterogeneity occurred via independent phenotypic drift of different properties. Since Dzarlieva *et al.* [1] and Peterson *et al.* [30] found that the rates of emergence of new tumor cell phenotypes can be as high as $\sim 10^{-2}$ per cell per generation, it was conceivable that subpopulations could have arisen, even in our short term experiments. Immediately after cloning, the numbers of cells were insufficient to examine experimentally until passage 3. However, by comparing cells from passage 3 and passage 5 we found that subcloned cell lines were identical in their experimental metastatic potentials,

suggesting that some stability remained at early passage numbers. We cannot be absolutely sure that each individual subclone remained genetically and phenotypically homogeneous, but diversification could be minimized using these procedures.

In our experiments phenotypic diversification occurred at disparate rates for different phenotypic properties. For example, subclones derived from MTF7 (T11) were relatively homogeneous in their growth rates and saturation densities; however, these same subclones were heterogeneous morphologically, and they possessed different experimental metastatic potentials, marker chromosomes and ploidy. These results indicated that by passage 11 clone MTF7 had diverged to form a mixed population of different tumor cells. By passage 35, cells from MTF7 subclones were heterogeneous for most of the phenotypes tested. The exception was the growth rate of MTF7 (T35) subclones, which were relatively homogeneous, exclusive of subclone MTF7 (T35).2, which had a doubling time of 26 h.

The divergence of multiple phenotypes in 13762NF mammary adenocarcinoma cell clones was not exclusive to clone MTF7. Examination of subclones derived from clones MTC and MTLn3 demonstrated that these clones also diverge to form multiple tumor cell subpopulations. Although subclones derived from clones MTC and MTLn3 were not tested as extensively as those from clone MTF7, their experimental metastatic potentials and growth rates *in vitro* indicated phenotypic diversification analogous to clone MTF7. Thus our data confirm the findings of others that tumor cell clones diverge phenotypically during *in vitro* tumor cell growth. In addition, we have demonstrated that multiple cellular phenotypes diverge independently as the cells are cultured, and in the accompanying paper we show that MTF7 subclones also diverge in their sensitivities to radiation, hyperthermia and FUdR [43].

A remaining paradox is the apparently random generation of tumor cell subpopulations and the suggestion that preprogrammed changes occur, as indicated by the reproducibility of phenotypic drift found in 13762NF cell clones. There are several possible explanations for this phenomenon. First, clonal cell divergence could be preprogrammed in a manner similar to embryonic development or normal cell diversification [22, 23]. Second, tumor clonal cell divergence could be random, but common selective pressures eliminate less 'fit' cell subpopulations, resulting in a mixture of cell populations with essentially predictable phenotypic traits. Third, one cell subpopulation may direct or modify another subpopulation's phenotype, such as metastatic potential or response to chemotherapy agents [12, 15, 16, 31, 33, 34]. Thus, the reproducibility of phenotypic drift could be the result of one or more subpopulations that 'control' other tumor cells and their pathways of phenotypic divergence.

Tumor cell phenotypic drift is defined as a change in a cell's phenotype as a function of proliferation [18]. Often this results in clonal divergence to form a heterogeneous tumor cell population. The observed drift in clonal properties with time appears to be the sum of individual 'subclonal' cell properties that, in addition, may be influenced by subclonal communication and control. Whether the phenotypic divergence seen in 13762NF cell clones is preprogrammed or random remains unknown, but in this system we have shown that phenotypic drift is reproducible.

Our results confirm some of Foulds' [5–7] hypotheses at the cellular level. Clonal divergence of multiple cell phenotypes by independent assortment, concomitant with progressive, continual evolution of a population's composite phenotype, is implicit in the data presented here. That the progeny of a cell clone acquire changes

that are permanent and irreversible, as hypothesized by Foulds [5, 6], could be considered questionable in light of the generation of tumor cell subpopulations with qualitatively and quantitatively different phenotypes than the original cell population. Although there is no direct molecular explanation for these phenomena, the 13672NF model system provides one means of defining and studying the cellular properties important in tumor diversification and progression.

Acknowledgments

Supported by U.S.P.H.S. National Cancer Institute grant RO1-CA28844 to G. L. Nicolson and the John A. Beck scholarship to D. R. Welch. We gratefully acknowledge the secretarial assistance of E. Felonia, P. Bramlett and A. Brodginski. This paper is submitted in partial fulfilment of the requirement for the Ph.D. degree at the University of Texas and appears as part of the copyrighted dissertation entitled 'Tumor Progression: Analysis of the Instability of the Metastatic Phenotype, Sensitivity to Radiation and Chemotherapy', by D. R. Welch.

References

[1] Dzarlieva, R., Schirrmacher, V., and Fusenig, N. F., 1982, Cytogenetic changes during tumor progression towards invasion, metastasis and immune escape in the EB/ESb model system. *International Journal of Cancer*, **30,** 633–642.

[2] Fidler, I. J., 1973, The relationship of embolic homogeneity, number, size, and viability to the incidence of experimental metastasis. *European Journal of Cancer*, **9,** 223–227.

[3] Fidler, I. J., and Nicolson, G. L., 1981, Immunobiology of experimental metastatic melanoma. *Cancer Biology Reviews*, Volume 2, edited by J. J. Marchalonis, M. G. Hanna and I. J. Fidler (New York: Marcel Dekker), pp. 171–234.

[4] Fialkow, P. J., 1979, Clonal origin of human tumors. *Annual Review of Medicine*, **30,** 135–176.

[5] Foulds, L., 1956, The histologic analysis of mammary tumors of mice. I. Scope of investigations and general principles of analysis. *Journal of the National Cancer Institute*, **17,** 701–712.

[6] Foulds, L., 1956, The histologic analysis of mammary tumors of mice. *Journal of the National Cancer Institute*, **17,** 713–754.

[7] Foulds, L., 1958, The natural history of cancer. *Journal of Chronic Diseases*, **8,** 2–18.

[8] Foulds, L., editor, 1975, *Neoplastic Development* (New York: Academic Press).

[9] Greig, R. G., Caltabiano, L., Reid, R., Field, F., and Poste, G., 1983, Heterogeneity of protein phosphorylation in metastatic variants of B16 melanoma. *Cancer Research*, **43,** 6057–6065.

[10] Hart, I. R., and Fidler, I. J., 1981, The implications of tumor heterogeneity for studies on the biology and therapy of cancer metastasis. *Biochimica et Biophysica Acta*, **651,** 37–50.

[11] Heppner, G. H., 1984, Tumor heterogeneity. *Cancer Research*, **44,** 2259–2265.

[12] Heppner, G. H., and Miller, B. E., 1983, Tumor heterogeneity: biological implications and therapeutic consequences. *Cancer Metastasis Reviews*, **2,** 5–23.

[13] Kawaguchi, T., Kawaguchi, M., Miner, K. M., Lembo, T. M., and Nicolson, G. L., 1983, Brain meninges tumor formation by *in vivo*-selected metastasis B16 melanoma variants in mice. *Clinical and Experimental Metastasis*, **3,** 247–259.

[14] Liotta, L. A., Kleinerman, J. and Saidel, G. M., 1976, The significance of hematogenous tumor cell clumps in the metastatic process. *Cancer Research*, **36,** 889–894.

[15] Miller, B. E., Miller, F. R., Leith, J., and Heppner, G. H., 1980, Growth interaction *in vivo* between tumor subpopulations derived from a single mouse mammary tumor. *Cancer Research*, **40,** 3977–3881.

[16] Miner, K. M., Kawaguchi, T., Uba, G. W., and Nicolson, G. L., 1982, Clonal drift of cell surface, melanogenic and experimental metastatic properties of *in vivo*-selected brain meninges-colonizing murine B16 melanoma. *Cancer Research*, **42,** 4631–4636.

[17] MINER, K. M., KLOSTERGAARD, J., GRANGER, G. A., and NICOLSON, G. L., 1983, Differences in cytotoxic effects of activated murine peritoneal macrophages and J774 monocytic cells on metastatic variants of B16 melanoma. *Journal of the National Cancer Institute*, **70,** 717–724.

[18] NERI, A., and NICOLSON, G. L., 1981, Phenotypic drift of metastatic and cell-surface properties of mammary adenocarcinoma cell clones during growth *in vivo*. *International Journal of Cancer*, **28,** 731–738.

[19] NERI, A., WELCH, D. R., KAWAGUCHI, T., and NICOLSON, G. L., 1982, The development and biological properties of malignant cell sublines and clones of a spontaneously metastasizing rat mammary adenocarcinoma. *Journal of the National Cancer Institute*, **63**(3), 507–517.

[20] NICOLSON, G. L., 1982, Cancer metastasis: Organ colonization and the cell surface properties of malignant cells. *Biochimica et Biophysica Acta*, **695,** 113–176.

[21] NICOLSON, G. L., 1984, Cell surface molecules and tumor metastasis. Regulation of metastatic diversity. *Experimental Cell Research*, **150,** 3–22.

[22] NICOLSON, G. L., 1984, Generation of phenotypic diversity and progression in metastatic tumors. *Cancer Metastasis Reviews*, **3,** 25–42.

[23] NICOLSON, G. L., 1984, Tumor progression, oncogenes and the evolution of metastatic phenotypic diversity. *Clinical and Experimental Metastasis*, **2,** 85–105.

[24] NICOLSON, G. L., and POSTE, G., 1982, Tumor cell diversity and host response in cancer metastasis. I. Properties of metastatic cells. *Current Problems in Cancer*, **7,** 1–83.

[25] NICOLSON, G. L., and POSTE, G., 1983, Tumor cell diversity and host responses in cancer metastasis. II. Host immune responses and therapy of metastases. *Current Problems in Cancer*, **7**(7), 1–43.

[26] NICOLSON, G. L., and POSTE, G., 1983, Tumor implantation and invasion at metastatic sites. *International Review of Experimental Pathology*, **25,** 77–181.

[27] NOWELL, P. C., 1976, The clonal evolution of tumor cell populations. *Science*, **194,** 23–28.

[28] NOWELL, P. C., 1983, Tumor progression and clonal evolution: The role of genetic instability. *Chromosome Mutation and Neoplasia*, edited by J. German (New York: A. R. Liss), pp. 413–432.

[29] PEARCE, V., PATHAK, S., MELLARD, D., WELCH, D. R., and NICOLSON, G. L., 1984, Chromosome and DNA analysis of rat 13762NF mammary adenocarcinoma cell lines and clones of different metastatic potentials. *Clinical and Experimental Metastasis*, **2,** 271–286.

[30] PETERSON, J. A., CERIANI, R. L., BLANK, E. W., and OSVALDO, L., 1983, Comparison of rates of phenotypic variability in surface antigen expression in normal and cancerous human breast epithelial cells. *Cancer Research*, **43,** 4291–4296.

[31] POSTE, G., 1982, Experimental systems for analysis of the malignant phenotype. *Cancer Metastasis Reviews*, **1,** 141–199.

[32] POSTE, G., BUCANA, C., RAZ, A., BUGELSKI, P., KIRSH, R., and FIDLER, I. J., 1982, Analysis of the fate of systemically administered liposomes and implications for their use in drug delivery. *Cancer Research*, **42,** 1412–1422.

[33] POSTE, G., DOLL, J., BROWN, A. E., TZENG, J., and ZEIDMAN, I., 1982, A comparison of the metastatic properties of B16 melanoma clones isolated from cultured cell lines, subcutaneous tumors and individual lung metastases. *Cancer Research*, **41,** 2770–2778.

[34] POSTE, G., DOLL, J., and FIDLER, I. J., 1981, Interactions among clonal subpopulations affect stability of the metastatic phenotype in polyclonal populations of B16 melanoma cells. *Proceedings of the National Academy of Sciences, U.S.A.*, **78,** 6226–6230.

[35] POSTE, G., and GREIG, R., 1982, On the genesis and regulation of cellular heterogeneity in malignant tumors. *Invasion and Metastasis*, **2,** 137–176.

[36] RAZ, A., 1984, The demonstration of nonlinear development of experimental tumor lung metastases. *Clinical and Experimental Metastasis*, **2,** 5–14.

[37] READING, C. L., KRAEMER, P. M., MINER, K. M., and NICOLSON, G. L., 1983, *In vivo* and *in vitro* properties of malignant variants of RAW117 metastatic murine lymphoma/lymphosarcoma. *Clinical and Experimental Metastasis*, **1,** 135–151.

[38] SCHIRRMACHER, V., 1980, Shifts in tumor cell phenotypes induced by signals from the microenvironment. Relevance for the immunobiology of cancer metastasis. *Immunobiology*, **157,** 89–98.

[39] STECK, P. A., and NICOLSON, G. L., 1983, Cell surface glycoproteins of 13762NF mammary adenocarcinoma clones of differing metastatic potentials. *Experimental Cell Research*, **147**, 255–267.

[40] TANIGAWA, N., MIZUNO, Y., HASHIMURA, T., HONDA, K., SATOMURA, K., HIKASA, Y., NIWA, O., SUGAHARA, T., YOSHIDA, O., KERN, D. H., and MORTON, D. L., 1984, Comparison of drug sensitivity among tumor cells within a tumor, between primary tumor and metastases, and between different metastases in the human tumor colony-forming assay. *Cancer Research*, **44**, 2309–2312.

[41] TOMASOVIC, S. P., THAMES, H. D. JR., and NICOLSON, G. L., 1982, Heterogeneity in hyperthermic sensitivities of rat 13762NF mammary adenocarcinoma cell clones of differing metastatic potentials. *Radiation Research*, **91**, 555–563.

[42] TSURUO, T., and FIDLER, I. J., 1981, Differences in drug sensitivity among tumor cells from parental tumors, selected variants, and spontaneous metastases. *Cancer Research*, **41**, 3058–3064.

[43] WELCH, D. R., EVANS, D. P., TOMASOVIC, S. P., MILAS, L., and NICOLSON, G. L., 1984, Multiple phenotypic divergence of mammary adenocarcinoma cell clones. II. Sensitivity to radiation, hyperthermia and FUdR. *Clinical and Experimental Metastasis*, **2**, 357–371.

[44] WELCH, D. R., MILAS, L., TOMASOVIC, S. P., and NICOLSON, G. L., 1983, Heterogeneous response and clonal drift of sensitivities of metastatic 13762NF mammary adenocarcinoma clones to gamma radiation *in vitro*. *Cancer Research*, **43**, 6–10.

[45] WELCH, D. R., NERI, A., and NICOLSON, G. L., 1983, Comparison of 'spontaneous' and 'experimental' metastasis using rat 13762 mammary adenocarcinoma metastatic cell clones. *Invasion and Metastasis*, **3**, 65–80.

[46] WELCH, D. R., and NICOLSON, G. L., 1983, Phenotypic drift and heterogeneity in response of metastatic mammary adenocarcinoma cell clones to adriamycin, 5-fluoro-2′-deoxyuridine and methotrexate treatment *in vitro*. *Clinical and Experimental Metastasis*, **1**, 317–325.